Radiat Med (2006) 24:202–209
DOI 10.1007/s11604-005-1528-y

ORIGINAL ARTICLE

Magnetic resonance cholangiopancreatography: comparison of respiratory-triggered three-dimensional fast-recovery fast spin-echo with parallel imaging technique and breath-hold half-Fourier two-dimensional single-shot fast spin-echo technique

Takayuki Masui · Motoyuki Katayama
Shigeru Kobayashi · Atsushi Nozaki
Masayoshi Sugimura · Mitsuru Ikeda
Harumi Sakahara

Received: July 5, 2005 / Accepted: November, 19, 2005

Abstract
Purpose. The aim of this study was to compare magnetic resonance cholangiopancreatography (MRCP) using respiratory-triggered (resp) three-dimensional Fourier transformation (3D) fast-recovery fast spin echo (FR-FSE) sequence with array spatial sensitivity technique (ASSET) for visualization of the pancreatobiliary system with breath-hold single thick-section and multiple thin-section MRCP using 2D single shot FSE (SSFSE) sequences.
Materials and methods. Forty patients underwent MRCP for evaluation of pancreatobiliary abnormalities in a 1.5-T magnet. Imaging time for resp 3D FR-FSE was recorded. The ghosting and blurring artifacts, overall image quality, and delineation of the pancreatobiliary ducts were evaluated using a five-point scale.
Results. On multisection 2D SSFSE source images, there were the least ghosting artifacts (4.9 ± 0.3, $P < 0.05$). Ghosting (3.4 ± 0.6, $P < 0.05$) and blurring (4.4 ± 0.8; $P < 0.05$) artifacts were the most prominent on resp 3D FR-FSE. 3D FR-FSE MRCP provided the highest rating of overall image quality (4.3 ± 0.8, $P < 0.05$) and delineation of third- and second-order branches of the hepatic ducts (2.9 ± 1.6 for third-order branches and 3.9 ± 1.3 for second-order branches, $P < 0.05$). Extrahepatic bile ducts, including upper and middle portions and cystic and pancreatic ducts, were also better seen with resp 3D FR-FSE MRCP than others.
Conclusion. MRCP with resp 3D FR-FSE using ASSET can be routinely used for acquiring information from the pancreatobiliary system.

Key words Pancreas, MR · Bile duct, MR · Gallbladder, MR

T. Masui (✉) · M. Katayama · S. Kobayashi
Department of Radiology, Seirei Hamamatsu General Hospital, 2-12-12 Sumiyoshi, Hamamatsu, Shizuoka 430-8558, Japan
Tel. +81-53-474-2222; Fax +81-53-474-8803
e-mail: masui@sis.seirei.or.jp

A. Nozaki
Application Research Group, General Electric Yokogawa Medical Systems, Hamamatsu, Japan

M. Sugimura
Division of Diagnostic Imaging Center, Seirei Hamamatsu General Hospital, Hamamatsu, Japan

M. Ikeda
Department of Medical Information and Medical Records, Nagoya University Hospital, Nagoya, Japan

H. Sakahara
Department of Radiology, Hamamatsu University School of Medicine, Hamamatsu, Japan

This article was presented at ISMRM in 2003.

Introduction

Magnetic resonance cholangiopancreatography (MRCP) has been widely used in the evaluation of the pancreatobiliary system.[1–4] So far many imaging techniques including three-dimensional Fourier transformation (3D) steady-state free procession (SSFP),[5] breath-hold or non-breath-hold two-dimensional (2D) fast spin-echo (FSE) sequences,[4,6] respiratory-triggered 3D FSE sequences,[3,7] 2D single-shot half Fourier type of FSE sequences (2D SSFSE)[1,2] have been used for

MRCP. The imaging strategies such as 2D thick single-section projection images, 2D thin multisection images, and 3D volume images acquired with or without breath-hold or respiratory triggering are now commonplace for MRCP. Each imaging technique has specific features. MRCP using 2D SSFSE can be obtained within 2 s, but this might be not sufficient to provide information for nondilated pancreatic ducts and high-order branches of the bile ducts.[1] Compared with the 2D SSFSE technique, the 3D technique with FSE can provide higher signal-to-noise ratios, and thinner imaging sections can be obtained. However, one of the major drawbacks for 3D FSE imaging is its very long acquisition time.[3]

Parallel imaging techniques using multicoils have been introduced[8,9]; and of these, the sensitivity encoding technique can be clinically used with commercially available multicoils. By shortening the acquisition time with parallel imaging techniques, spatial or temporal resolutions of images can be improved. Because the 3D FSE technique with respiratory triggering for MRCP has an inherently high signal-to-noise ratio, it can be combined with sensitivity encoding technique despite the penalty to the signal-to-noise ratio to visualize nondilated pancreatobiliary ducts. To compensate for the decrease in signal-to-noise ratios, the application of the 180° and –90° radiofrequency pulses at the end of the spin-echo sequence, so-called fast-recovery pulse should be considered.[10,11] When respiratory-triggered techniques are used, the k space should be filled during a short period at the end-respiratory phase to obtain images with fewer motion artifacts.

The purpose of the study was to assess the ability of respiratory-triggered 3D fast-recovery FSE with a sensitivity-encoding technique to visualize the higher-order branch of the bile duct and pancreatic ducts in comparison with thick single-projection MRCP and thin multisection MRCP using SSFSE.

Materials and methods

This study was performed within the guidelines of our institutional review board, and informed consent was obtained from each patient prior to the MR study. A total of 42 consecutive patients were referred for the MR evaluation of the pancreatobiliary abnormalities. Two patients were excluded because of triggering problems in the respiratory-triggered T2-weighted FSE technique prior to MRCP and did not undergo MRCP with the respiratory-triggered 3D fast-recovery FSE technique. Thus, 40 patients (26 men, 14 women; mean age 59 years, range, 20–86 years), were included in this study. The final diagnoses of the diseases of the patients were cholecystitis with gallstone in seven patients, cancer of the common bile duct in one, gallstone in two, stone in the intrahepatic bile duct in one, cholecystitis without gallstone in two, acute pancreatitis in two, chronic pancreatitis in one, cystic lesion of the pancreas in six, pancreatic cancer in three, congenital obstruction of the biliary tract with cholangitis in one, recurrence of the pancreatic or biliary tract cancer after pancrea toduodenectomy in three, status of pancreatoduodenectomy in one, hepatocellular carcinoma in two, chronic hepatitis in one, pancreatic divisum in one, no abnormality of pancreatobiliary system in six. These diagnoses were confirmed by computed tomography (CT), ultrasonography, endocanal retrograde cholangiopancreatography or operation followed by their clinical courses for more than six months.

Magnetic resonance imaging

All magnetic resonance (MR) imaging was performed with a 1.5-T system (Horizon LX EchoSpeed, software version 8.3; GE Medical Systems, Milwaukee, WI, USA) using a torso phased array multicoil after a fasting period of at least 4 h.

MRCP using respiratory-triggered 3D fast-recovery FSE sequence

Scans for MRCP using the respiratory-triggered 3D fast-recovery FSE sequence with array spatial sensitivity technique (ASSET; GE Medical Systems)[12] consisted of two parts: (1) reference scan for a sensitivity map in the field of view and (2) scan with respiratory-triggered 3D fast-recovery FSE sequence.

The reference scan was obtained using 2D fast multiplanar spoiled gradient-recalled acquisition in the steady state in a coronal plane covering the whole abdomen with the following parameters: TR/TE, 150/2.4 ms; flip angle 90°; field of view 40 × 40 cm; matrix 128 × 128 to 96 × 96; bandwidth 62.5 kHz; section thickness 5–10 mm; intersection gap 1–2 mm, and one signal acquired. The image time was 25 s.

Scans for MRCP were acquired in a coronal plane with the following imaging parameters: 3300–7800/475 (TR/effective TE); flip angle 90°; echo train length 123; echo space 8.4 ms; field of view 30 × 30 cm; matrix 256 × 224, with zero fill interpolation (ZIP) for 512 matrix; bandwidth 31.5 kHz; section thickness 2 mm; 76–144 sections with ZIP2 for slice direction; acquisition window for data sampling 25%; chemically selective fat saturation and image time 3–5 min. Voxel dimensions were nearly isotropic at 1.2 × 1.3 × 2.0 mm without ZIP.

MRCP using thick single-section SSFSE sequence

Scans for MRCP were acquired in a coronal plane with the following imaging parameters: infinite/975; flip angle 90°; echo train length 136; echo space 7.4 ms; field of view 24 × 24 to 30 × 30 cm; matrix, 256 × 256 to 320 × 320; bandwidth 31.5 kHz; section thickness 40–60 mm, chemically selective fat saturation and image time 2 s. Matrix size was 0.8 × 0.8 to 0.9 × 0.9 mm.

MRCP using thin multisection SSFSE sequence

Scans for MRCP were acquired in a coronal plane with the following imaging parameters; infinite/100; flip angle 90°; echo train length 110; echo space 6.7 ms; field of view 24 × 24 to 30 × 30 cm; matrix, 256 × 192; bandwidth, 62.5 kHz; section thickness 4 mm without intersection gap; chemically selective fat saturation and image time 1 s for one section; number of sections 20–36; matrix size 0.9 × 1.3 to 1.2 × 1.6 mm.

Imaging processing and evaluation

All source images were transferred to a workstation (Advantage Windows 3.1; GE Medical Systems). Postprocessing of the source images obtained with the respiratory-triggered 3D fast-recovery FSE sequence and the thin multisection SSFSE sequence was performed using multiplanar volume reformation with the maximum intensity projection (MIP). MIP images were obtained from the value of the section taken along lines perpendicular to it. Slice thickness of data for MIP images was 20–100 mm. Angle and range of the section thickness were freely changeable by the reader to visualize the pancreatobiliary system.

For the acquisition of 3D fast-recovery FSE and thin multisection SSFSE sequences, the number of the image sections and calculated nominal acquisition time and actual counted time were recorded. Source and MIP images with multiplanar volume reformation were obtained for each sequence and consisted of coronal images.

The two readers who were unaware of the patients' clinical history, utilized sequence, or results of the evaluations by the other observer independently reviewed each image on the display monitor in random order and evaluated the image quality regarding ghosting artifacts and blurring using a five-point scale.

Ghosting artifacts or blurring artifacts were ranked as: 1 (severe), where the anatomic structures were difficult to identify because of artifacts in the phase-encoding direction or because of blurring of the edges; 2 (moderate), where the definition of the anatomic structures was poor because of ghosting artifacts or blurring; 3 (mild), where lesser degrees of artifacts were noted than at the moderate level; 4 (minimal), rated subjectively between 3 and 5; or 5 (absent), where there were no ghosting artifacts or blurring.

Overall image quality was ranked as: 1 (poor), where a diagnosis could not be made due to motion or poor signal intensities of the structures; 2 (acceptable), where the images were diagnostic but there were moderate motion artifacts and poor signal-to-noise ratios; 3 (good), where there were some motion artifacts or poor signal-to-noise ratios, but less than at the acceptable level; 4 (moderate), where the image quality was subjectively rated between 3 and 5; or 5 (excellent), where there were no motion artifacts, and signal-to-noise ratios were good.

The delineation of the pancreatobiliary ducts was also evaluated regarding the following points: the first-, second-, and third-order intrahepatic bile ducts; the extrahepatic bile duct; upper one-third between the bifurcation of the left and right common hepatic duct and ampulla of the duodenum, middle and lower, the gallbladder, cystic duct, and pancreatic duct in the head, body, and tail. The following grading system was used: 5, excellent for complete delineation; 4, good for delineation of at least 90%; 3, fair for delineation of less than 90%; 2, poor for delineation; and 1, not visualized.

Statistical analysis

Qualitative ranks for overall image quality and delineation of pancreatobiliary ducts among three MRCP images were statistically compared using the Friedman test followed by the Steel-Dwass test. For the comparison of the ghosting artifacts and blurring artifacts between two modalities, the Wilcoxon signed rank test was used.

Results

Imaging time and number of sections

Respiratory triggered 3D fast-recovery FSE sequences

The mean nominal number of respiratory cycles was 15.7 ± 2.7 (mean rate ± SD) / min (range 10–21/min). The calculated mean duration of respiratory cycle was 3750 ms. The mean nominal imaging time was 3 min 29 s ± 49 s (range 2 min 15 s to 4 min 51 s). The mean actual imaging time was 3 min 57 s ± 64 s (range 2 min 20 s to 6 min 31 s). The mean prolongation of the imaging time was 14% ± 22%. The mean number of sections was 97 ±

Table 1. Image quality and artifacts on MRCP with three different sequences in 40 patients

	Ghosting artifact		Blurring		
Sequence	Source	MIP	Source	MIP	Overall quality
3D FSE	3.4 ± 0.6	3.7 ± 0.7	4.4 ± 0.8	4.8 ± 0.6	4.3 ± 0.8
2D Multi-SSFSE	4.9 ± 0.3†‡	4.3 ± 0.7†	4.6 ± 0.6†‡	4.9 ± 0.4†	3.8 ± 0.8†
2D Single SSFSE	4.0 ± 0.8†		4.9 ± 0.3†		3.7 ± 1.0†

MRCP, magnetic resonance cholangiopancreatography; 3D, 2D, three- and two-dimensional; FSE, fast spin echo; SSFSE, single-shot FSE
Results are the mean rank ± SD for the mean values from two readers' data. Ranks indicate the subjective rate: definitely present, or nondiagnostic (1) to definitely absent, or excellent (5). Source and MIP indicate the source or maximum intensity project images, respectively
† Significant difference against the 3DFSE value
‡ Significant difference against the 2D single SSFSE value

Table 2. Visualization of intrahepatic bile duct and common hepatic ducts on MRCP with three different sequences in 40 patients

Sequence	3rd-Order branches[a]	2nd-Order branches[a]	1st-Order branches[a]	Posterior branches[a]
3DFSE	2.9 ± 1.5	3.9 ± 1.3	4.6 ± 0.9	3.8 ± 1.5
2D Multi-SSFSE	2.4 ± 1.4†	3.3 ± 1.2†‡	4.2 ± 0.8†	3.4 ± 1.3†‡
2D Single SSFSE	2.0 ± 1.3†	2.9 ± 1.0†	3.9 ± 1.0†	2.7 ± 1.1†

Results are the mean rank ± SD for the mean values from two observers' data. Ranks indicate the subjective rate, definitely absent (1) to definitely present (5)
[a] Third-, second-, and first-order branches of the hepatic ducts, respectively. Posterior indicates the posterior branch of the hepatic duct
† Significantly different from the value for 3DFSE
‡ Significantly different from the value for 2D single SSFSE

18 (range 76–144). All cases were diagnostic, but prior to MRCP sequences respiratory-triggered T2-weighted FSE images were obtained.

Thin multisection 2D SSFSE sequences

The mean imaging time was 43 ± 6 s (range 32–59 s). The mean number of obtained sections was 26 ± 3 (range 20–36). In all cases, The breath-holding maneuver for imaging was repeated twice.

Image quality

In all the 40 patients included in the study, all of the images with three MRCP sequences were diagnostic. In 2D multisection SSFSE source images, ghosting artifacts such as noise were least identified among the three sequences (mean rate ± SD, 4.9 ± 0.3, $P < 0.05$) (Table 1). The source image of respiratory-triggered 3D fast-recovery FSE provided the lowest rating regarding the artifacts (3.4 ± 0.6). Blurring effects due to motion were prominent in the respiratory-triggered method (4.4 ± 0.8) because of physiological changes in the duration of the respiratory cycle during the imaging acquisition and/or the variable depth of the respiration. In such cases, less visualization of the intrahepatic and pancreatic ducts was noted (Fig. 1). Unstable breath-holding caused misregistration artifacts on MRCP using multisection 2D SSFSE sequence (Fig. 1). However, in general, among the three types of MRCP from respiratory-triggered 3D fast-recovery FSE and multiple- and single-section 2D SSFSE images, the respiratory-triggered method provided the highest rating of the overall quality of images (4.3 ± 0.8, $P < 0.05$) (Figs. 2, 3).

Visualization of pancreatobiliary ducts

Intrahepatic bile ducts were well visualized with the 3D FSE technique among the three MRCP sequences (2.9 ± 1.5 for third-order branches, 3.9 ± 1.3 for second-order branches, and 4.6 ± 0.9 for first-order branches with 3D FSE, respectively ($P < 0.05$) (Table 2; Figs. 2, 3). Single-section MRCP with the current sequence provided lower confidence levels in the visualization of the first- to third-order branches of the hepatic ducts ($P < 0.05$). Upper and middle portions of the common bile ducts and the cystic duct were visualized best with MRCP using the 3D FSE sequence ($P < 0.05$) (Table 3), and pancreatic ducts

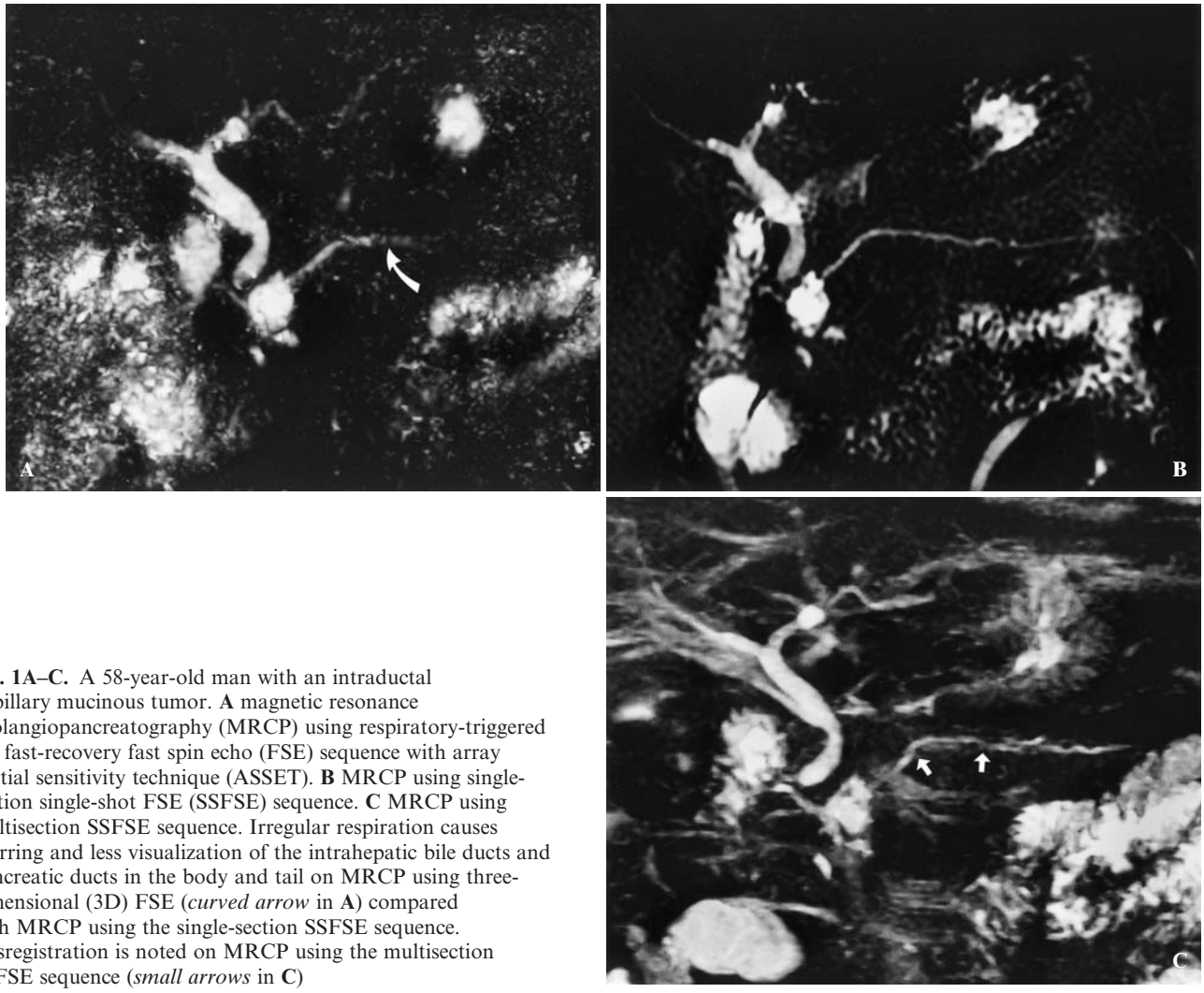

Fig. 1A–C. A 58-year-old man with an intraductal papillary mucinous tumor. **A** magnetic resonance cholangiopancreatography (MRCP) using respiratory-triggered 3D fast-recovery fast spin echo (FSE) sequence with array spatial sensitivity technique (ASSET). **B** MRCP using single-section single-shot FSE (SSFSE) sequence. **C** MRCP using multisection SSFSE sequence. Irregular respiration causes blurring and less visualization of the intrahepatic bile ducts and pancreatic ducts in the body and tail on MRCP using three-dimensional (3D) FSE (*curved arrow* in **A**) compared with MRCP using the single-section SSFSE sequence. Misregistration is noted on MRCP using the multisection SSFSE sequence (*small arrows* in **C**)

in the body and tail were also best demonstrated with the 3D FSE technique (3.8 ± 1.6 for the body and 3.7 ± 16 for the tail, $P < 0.05$) (Table 4).

Discussion

The current study demonstrated the superiority of the respiratory-triggered 3D fast-recovery FSE sequence for MRCP with ASSET. MRCP is now accepted as one of the standard MR techniques for noninvasive evaluation of the pancreatobiliary tracts.[1–4] The 2D SSFSE sequence was widely used for MRCP because of the very short acquisition time, mainly to evaluate extrahepatic bile and pancreatic ducts and the gallbladder.[1,2]

Three-dimensional volume acquisitions have been introduced using FSE, gradient echo, and echo planar methods.[3,5,13] Several articles have suggested the high clinical value of MRCP with the respiratory-triggered 3D FSE technique.[3,7] However, long acquisition times of approximately 6–10 min have been a major obstacle to the routine use of 3D MRCP acquisitions.[3] A parallel imaging approach is one of the promising ways of overcoming the major obstacle to 3D MRCP. In this study, the array spatial sensitivity technique (ASSET, GE Medical Systems)[12] of parallel imaging techniques was used with commercially available torso phased array multicoils. With the currently available software (Signa LX, version 8.3) for respiratory-triggered 3D FSE sequence, the data acquisition window was approximately 25%–30% of one respiratory cycle. To keep the scan time shorter, the matrix should be reduced to be 256×128 or less. With ASSET, which is applied to phase-encoded directions, a matrix such as 256×224 can be maintained without prolongation of the imaging time.

The actual imaging time for respiratory-triggered 3D FSE increased by approximately 15% of the nominal imaging time, which was calculated from the respiratory

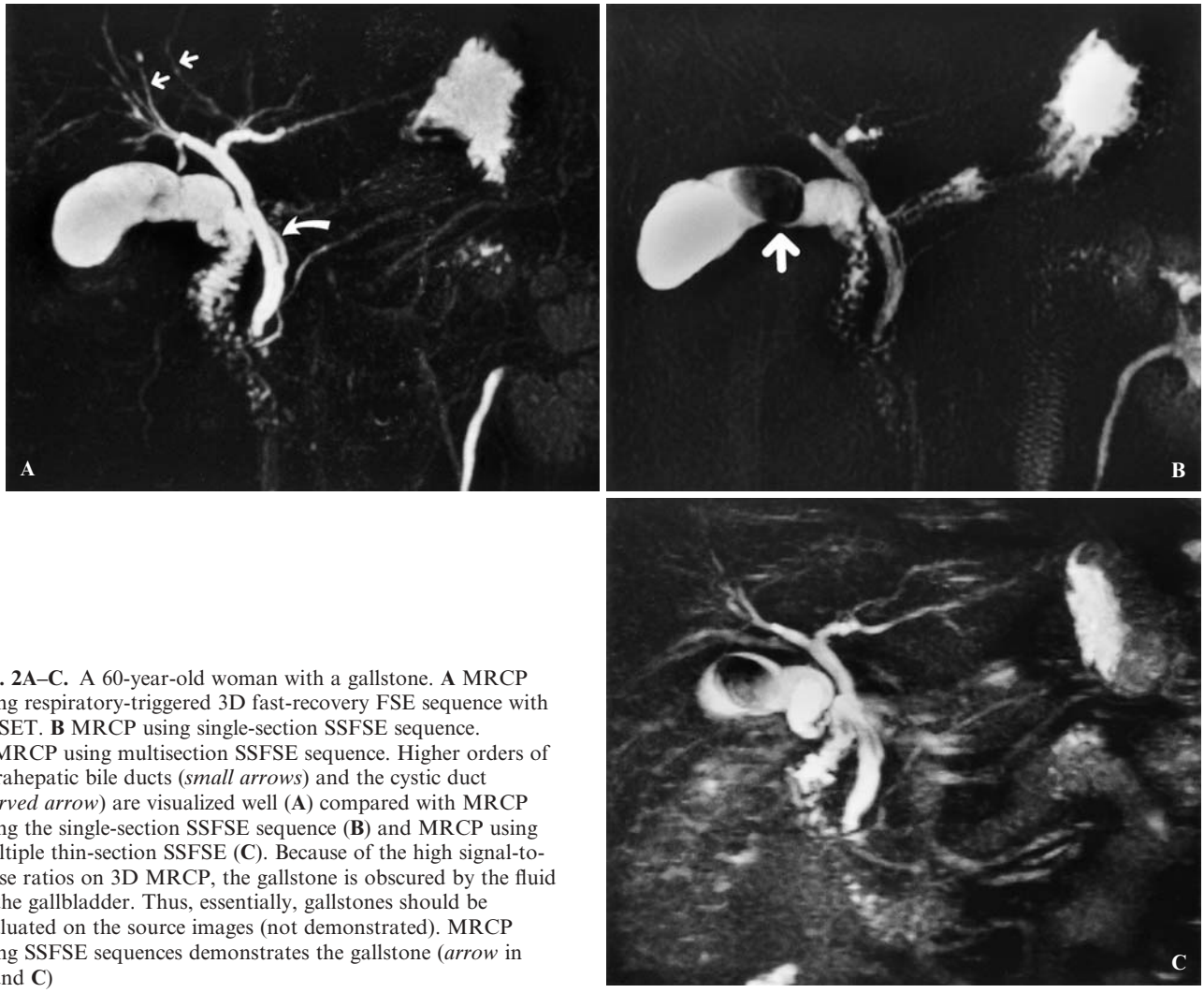

Fig. 2A–C. A 60-year-old woman with a gallstone. **A** MRCP using respiratory-triggered 3D fast-recovery FSE sequence with ASSET. **B** MRCP using single-section SSFSE sequence. **C** MRCP using multisection SSFSE sequence. Higher orders of intrahepatic bile ducts (*small arrows*) and the cystic duct (*curved arrow*) are visualized well (**A**) compared with MRCP using the single-section SSFSE sequence (**B**) and MRCP using multiple thin-section SSFSE (**C**). Because of the high signal-to-noise ratios on 3D MRCP, the gallstone is obscured by the fluid in the gallbladder. Thus, essentially, gallstones should be evaluated on the source images (not demonstrated). MRCP using SSFSE sequences demonstrates the gallstone (*arrow* in **B** and **C**)

Table 3. Visualization of extrahepatic bile ducts and gallbladder on MRCP with three different sequences in 40 patients

Sequence	Upper[a]	Middle[a]	Lower[a]	Cystic[a]	Gallbladder
3DFSE	4.7 ± 1.0	4.4 ± 1.3	4.0 ± 1.5	3.7 ± 1.6	3.8 ± 1.7
2D Multi-SSFSE	4.2 ± 1.2[†]	4.1 ± 1.3[†]	3.9 ± 1.4	3.2 ± 1.5[†]	4.0 ± 1.6[‡]
2D Single SSFSE	3.9 ± 1.0[†]	3.8 ± 1.5[†]	3.5 ± 1.6[†]	2.7 ± 1.3[†]	3.2 ± 1.7[†]

Results are the mean rank ± SD for the mean values from two observers' data. Ranks indicate the subjective rate, definitely absent (1) to definitely present (5)

[a] Upper, middle, and lower indicate the third of the upper, middle, and lower portions of the extrahepatic bile duct, respectively

[†] Significantly different from the value for 3DFSE

[‡] Significantly different from the value for 2D single SSFSE

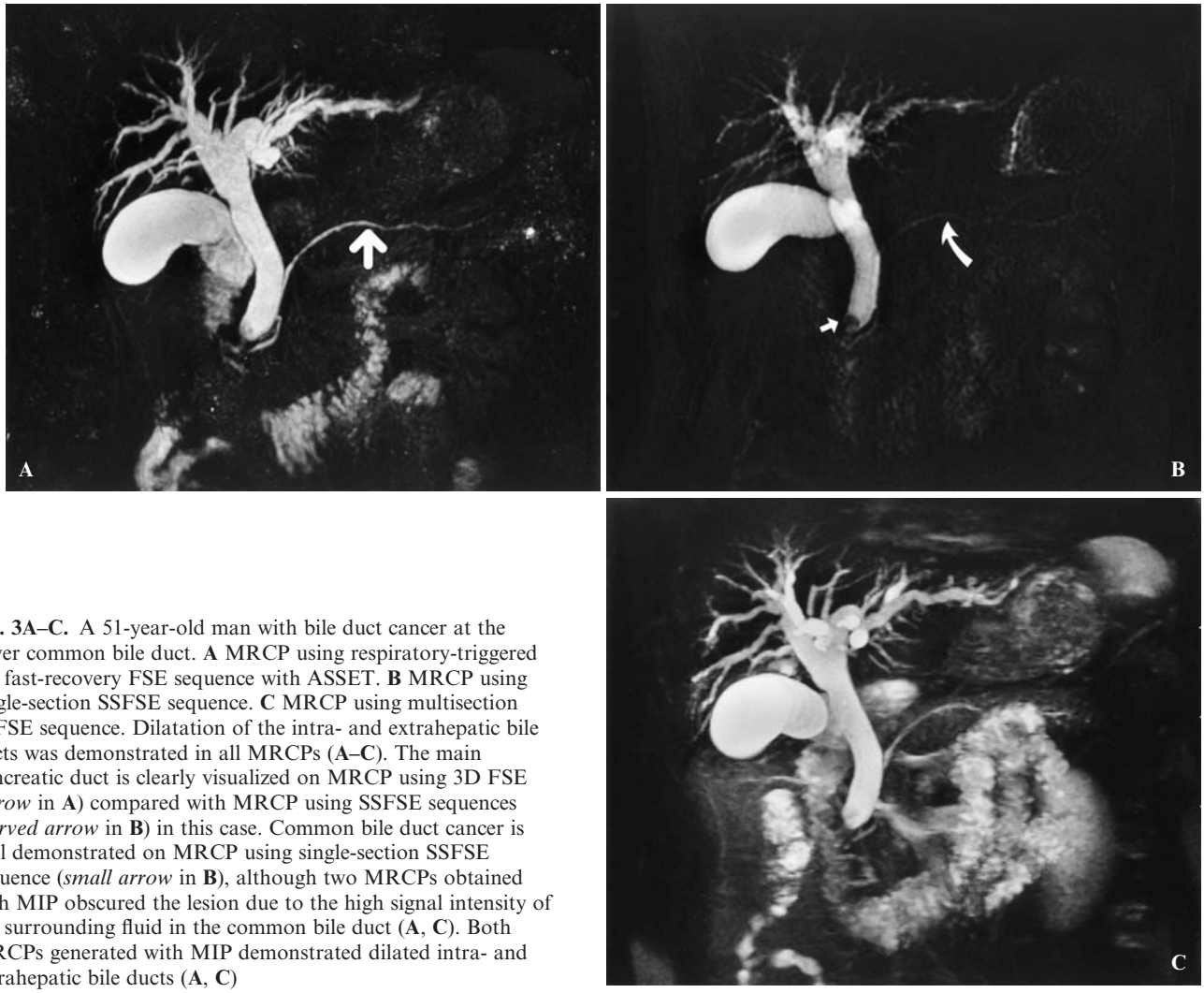

Fig. 3A–C. A 51-year-old man with bile duct cancer at the lower common bile duct. **A** MRCP using respiratory-triggered 3D fast-recovery FSE sequence with ASSET. **B** MRCP using single-section SSFSE sequence. **C** MRCP using multisection SSFSE sequence. Dilatation of the intra- and extrahepatic bile ducts was demonstrated in all MRCPs (**A–C**). The main pancreatic duct is clearly visualized on MRCP using 3D FSE (*arrow* in **A**) compared with MRCP using SSFSE sequences (*curved arrow* in **B**) in this case. Common bile duct cancer is well demonstrated on MRCP using single-section SSFSE sequence (*small arrow* in **B**), although two MRCPs obtained with MIP obscured the lesion due to the high signal intensity of the surrounding fluid in the common bile duct (**A**, **C**). Both MRCPs generated with MIP demonstrated dilated intra- and extrahepatic bile ducts (**A**, **C**)

Table 4. Visualization of pancreatic ducts on MRCP with three different sequences in 40 patients

Sequence	Head[a]	Body[a]	Tail[a]	Santolini	2nd Order
3DFSE	3.7 ± 1.6	3.8 ± 1.6	3.7 ± 1.6	1.5 ± 1.0	1.4 ± 1.1
2D Multi-SSFSE	3.5 ± 1.3	3.5 ± 1.2[†]	3.2 ± 1.4[†]	1.5 ± 1.0	1.4 ± 1.0
2D Single SSFSE	3.4 ± 1.4	3.3 ± 1.4[†]	2.8 ± 1.5[†]	1.4 ± 0.9	1.3 ± 1.0

Results are the mean rank ± SD for the mean values from two observers' data. Ranks indicate the subjective rate: definitely absent (1) to definitely present (5)
[†] Significantly different from the value for 3DFSE
[‡] Significantly different from the value for 2D single SSFSE

rate just before the start of the acquisition. This result was consistent with the previous published data.[3]

The 3D sequence provides the merit of a high signal-to-noise ratio even with thin sections. By using ASSET, the signal-to-noise ratio decreases to some extent, which depends on the reduction factor for parallel imaging and geometric factor of coil elements.[8] One of the ways to increase the signal-to-noise ratios of the fluid is application of the fast-recovery pulse, 180° and –90° radiofrequency pulses to the end of the FSE sequence.[10,11]

Currently, in 2 of 42 patients, respiratory-triggered 3D MRCP was not performed due to failure of the prior respiratory-triggered T2-weighted FSE. In the other 40 patients, three MRCPs were successfully performed, and

all image quality was diagnostic. Because of their very short imaging time, approximately within 2 s, the ghosting and blurring artifacts of the source images of multisection SSFSE and projection SSFSE images were less prominent than that of respiratory-triggered 3D FSE. Among three types of MRCP, the overall image quality of MRCP using the respiratory-triggered 3D fast recovery FSE sequence with ASSET was best in the current study probably due to the higher signal-to-noise ratio of the panceatobiliary ducts, although on the current version (8.3), artifacts on the source images of respiratory-triggered 3D FSE sequence with ASSET were rather prominent. Because of the background reduction of the signal-to-noise ratios and visualization of the fluid in the smaller branches such as second- and third-order intrahepatic bile duct, recognition of the intrahepaptic bile duct was significantly better than in the other two MRCPs. As noted in Figs. 2 and 3, MRCP, which is generated with MIP, might obscure stone or lesion in the bile duct or gallbladder. To evaluate the small lesions in the ducts and gallbladder, review of the source images may be essential especially when 3D acquisition of the images is performed.

Because of the large coverage of the imaging volume with high spatial resolution, MRCP using the respiratory-triggered fast-recovery 3D FSE sequence provides better visualization of the hepatic duct in any direction of projection of MRCP. We did not directly compare the multidirectional projection MRCP generated from the 3D FSE data set with other SSFSE MRCPs. After one acquisition of the 3D FSE, postprocessing can be effectively performed. Multisection SSFSE suffered from misregistration effects of side-by-side slices.[1] Projection images were essential for evaluation of the continuity of the pancreatic duct, but overlap of these images was problematic, and multiprojection images should be obtained. Theoretically, respiratory-triggered methods cause the blurring effects and provide summation of the event only during imaging time.

In conclusion, MRCP using the respiratory-triggered fast recovery 3D FSE sequence with ASSET provides better information about higher-order intrahepatic bile ducts than MRCP with other 2D SSFSE sequences. By using ASSET, this method may be used in clinical settings and provides more information than others.

References

1. Masui T, Takehara Y, Ichijo K, et al. Evaluation of the pancreas: a comparison of single thick-slice MR cholangiopancreatography with multiple thin-slice volume reconstruction MR cholangiopancreatography. AJR Am J Roentgenol 1999;173:1519–26.
2. Miyazaki T, Yamashita Y, Tsuchigame T, et al. MR cholangiopancreatography using HASTE (half-Fourier acquisition single-shot turbo spin-echo) sequences. AJR Am J Roentgenol 1996;166:1297–303.
3. Soto JA, Barish MA, Yucel EK, et al. Pancreatic duct: MR cholangiopancreatography with a three-dimensional fast spin-echo technique. Radiology 1995;196:459–64.
4. Takehara Y, Ichijo K, Tooyama N, et al. Breath-hold MR cholangiopancreatography with a long-echo-train fast spin-echo sequence and a surface coil in chronic pancreatitis. Radiology 1994;192:73–8.
5. Wallner BK, Schumacher KA, Weidenmaier W, et al. Dilated biliary tract: evaluation with MR cholangiography with a T2-weighted contrast-enhanced fast sequence. Radiology 1991;181:805–8.
6. Guibaud L, Bret PM, Reinhold C, et al. Bile duct obstruction and choledocholithiasis: diagnosis with MR cholangiography. Radiology 1995;197:109–15.
7. Barish MA, Yucel EK, Soto JA, et al. MR cholangiopancreatography: efficacy of three-dimensional turbo spin-echo technique. AJR Am J Roentgenol 1995;165:295–300.
8. Pruessmann KP, Weiger M, Scheidegger MB, et al. SENSE: sensitivity encoding for fast MRI. Magn Reson Med 1999; 42:952–62.
9. Sodickson DK, Griswold MA, Jakob PM. SMASH imaging. Magn Reson Imaging Clin N Am 1999;7:237–54, vii–viii.
10. Katayama M, Masui T, Kobayashi S, et al. Fat-suppressed T2-weighted MRI of the liver: comparison of respiratory-triggered fast spin-echo, breath-hold single-shot fast spin-echo, and breath-hold fast-recovery fast spin-echo sequences. J Magn Reson Imaging 2001;14:439–49.
11. Masui T, Katayama M, Kobayashi S, et al. T2-weighted MRI of the female pelvis: comparison of breath-hold fast-recovery fast spin-echo and nonbreath-hold fast spin-echo sequences. J Magn Reson Imaging 2001;13:930–7.
12. Karnick A, King K. SENSE geometry factor image processing. In: Proceedings of the International Society for Magnetic Resonance in Medicine. Scotland; 2001. p. 1801.
13. Wielopolski PA, Gaa J, Wielopolski DR, et al. Breath-hold MR cholangiopancreatography with three-dimensional, segmented, echo-planar imaging and volume rendering. Radiology 1999;210:247–52.